Gondwana Research 28 (2015) 1183–1196

Contents lists available at ScienceDirect

Gondwana Research

journal homepage: www.elsevier.com/locate/gr

U–Pb age of the coesite-bearing eclogite from NW Borborema Province, NE Brazil: Implications for western Gondwana assembly

Ticiano José Saraiva dos Santos [a,*], Wagner da Silva Amaral [a], Matheus Fernando Ancelmi [a,b], Michele Zorzetti Pitarello [a,d], Reinhardt Adolfo Fuck [c], Elton Luiz Dantas [c]

[a] Geosciences Institute, State University of Campinas — UNICAMP, P.O. box 6152, 13083-970 Campinas, SP, Brazil
[b] Science and Technology Institute, Federal University of Alfenas, Poços de Caldas, MG, Brazil
[c] Geosciences Institute, University of Brasília, Brasília, DF, Brazil
[d] CPRM — Geological Survey of Brazil, Manaus, AM, Brazil

ARTICLE INFO

Article history:
Received 26 February 2014
Received in revised form 12 September 2014
Accepted 17 September 2014
Available online 14 October 2014

Handling Editor: Z.M. Zhang

Keywords:
Borborema Province
UHP rocks
Suture zone
Coesite-bearing eclogite
Gondwana assembly

ABSTRACT

The Late Neoproterozoic assembly of western Gondwana played an important role in the subduction of oceanic and continental lithospheres. Such event was also a source of arc magmatism, reworking of cratonic margins and development of ultra-high pressure (UHP) suture zones. In the Borborema province, NE Brazil, we have described for the first time UHP rocks enclosed within gneiss migmatite and calc-silicate rocks. They bear coesite included in atoll-type garnet from metamafic rocks, identified by petrographic study and Raman microspectroscopy analysis. U–Pb zircon dating of the leucosome of the migmatites and the calc-silicate rock displays, concordant ages of 639 ± 10 Ma and 649.7 ± 5 Ma, respectively, here interpreted as the minimum age of the eclogitization event in the region. U–Pb zircon dating of the coesite-bearing rock defined a concordia age of 614. 9 ± 7.9 Ma that comprised the retrograde eclogitic conditions to amphibolite facies. The UHP rocks, mostly retrograded to garnet amphibolites, occur enclosed in the Paleoproterozoic continental block composed of calc-silicate rocks, migmatized sillimanite gneiss, mylonitic augen gneiss and granitic and tonalitic gneiss along a narrow N–S oriented belt between the Santa Quitéria magmatic arc and the Transbrasiliano lineament. This block was involved in the subduction to UHP eclogite depths, and was retrogressed to amphibolite during its exhumation and thrusting. Our data indicate an important Neoproterozoic transcontinental suture zone connecting the Pharusian belt with Borborema Province, and probably with the Brasília belt in central Brazil.

1. Introduction

One of the basic questions in global tectonics is to determine the location of old suture zones. On the eastern margin of the West Africa craton a Pan-African suture zone is evident in northern Mali, Togo, Benin, and Ghana due to the presence of remnants of oceanic crust, arc magmatism, and ultra-high pressure (UHP) rocks, also attested by geophysical data (Lesquer et al., 1984; Caby, 1989; Affaton et al., 1991; El-Hadj Tidjani et al., 1997; Jahn et al., 2001; Duclaux et al., 2006). Several studies have proposed a correlation between the Pharusian belt and the Borborema Province, in which two transcontinental lineaments, the Transbrasiliano in Brazil and the Hoggar 4°50 — Kandi in Africa, comprise the first-order correlation (Fig. 1A) (Castaing et al., 1994; Trompette, 1994; Brito Neves et al., 2002; Arthaud et al., 2008; Santos et al., 2008a; Kalsbeek et al., 2012; Archanjo et al., 2013; Cordani et al., 2013a,b).

Occurrence of high-pressure (HP) and UHP rocks, particularly associated with coesite-bearing eclogite, is important in the reconstruction of supercontinents, providing information on lithosphere subduction, residence and exhumation processes (Maruyama et al., 1996; Carswell and Zhang, 1999; Ernst, 2001). Uncontested Neoproterozoic suture zones are well defined in Africa, mainly by the occurrence of HP and UHP mafic and ultramafic rocks (Caby, 2003 and references therein). In contrast, suture zones in Brazil remain unclear, mainly due to the lack of UHP rocks, which led to interpretations of these zones bordering the São Luís craton (Trompette, 2000) or connecting with the Araguaia belt (Fig. 1A) (Tohver et al., 2006; Cordani et al., 2009) or assumed to being buried beneath the Phanerozoic Parnaíba basin where some high density gravity anomalies may represent hidden remnants of an oceanic suture (Lesquer et al., 1984; Fetter et al., 2003).

While the understanding of such features is provided by HP-UHP rocks, dating of a UHP metamorphic peak using the U–Pb method is problematic, mainly due to the closure temperatures of some minerals, such as sphene and rutile, which are usually lower than those of the metamorphic peak.

In central Brazil, remnants of an Early Neoproterozoic oceanic crust and a Neoproterozoic magmatic arc (Pimentel et al., 1991; Pimentel and

* Corresponding author at: Universidade Estadual de Campinas-UNICAMP, Instituto de Geociências - Rua: Joao Pandiá Calógeras, 51, Cidade Universitaria, CEP: 13083-970, P.O.Box 6152, Campinas-São Paulo, Brasil.
E-mail address: ticiano@ige.unicamp.br (T.J.S. dos Santos).

http://dx.doi.org/10.1016/j.gr.2014.09.013
1342-937X/

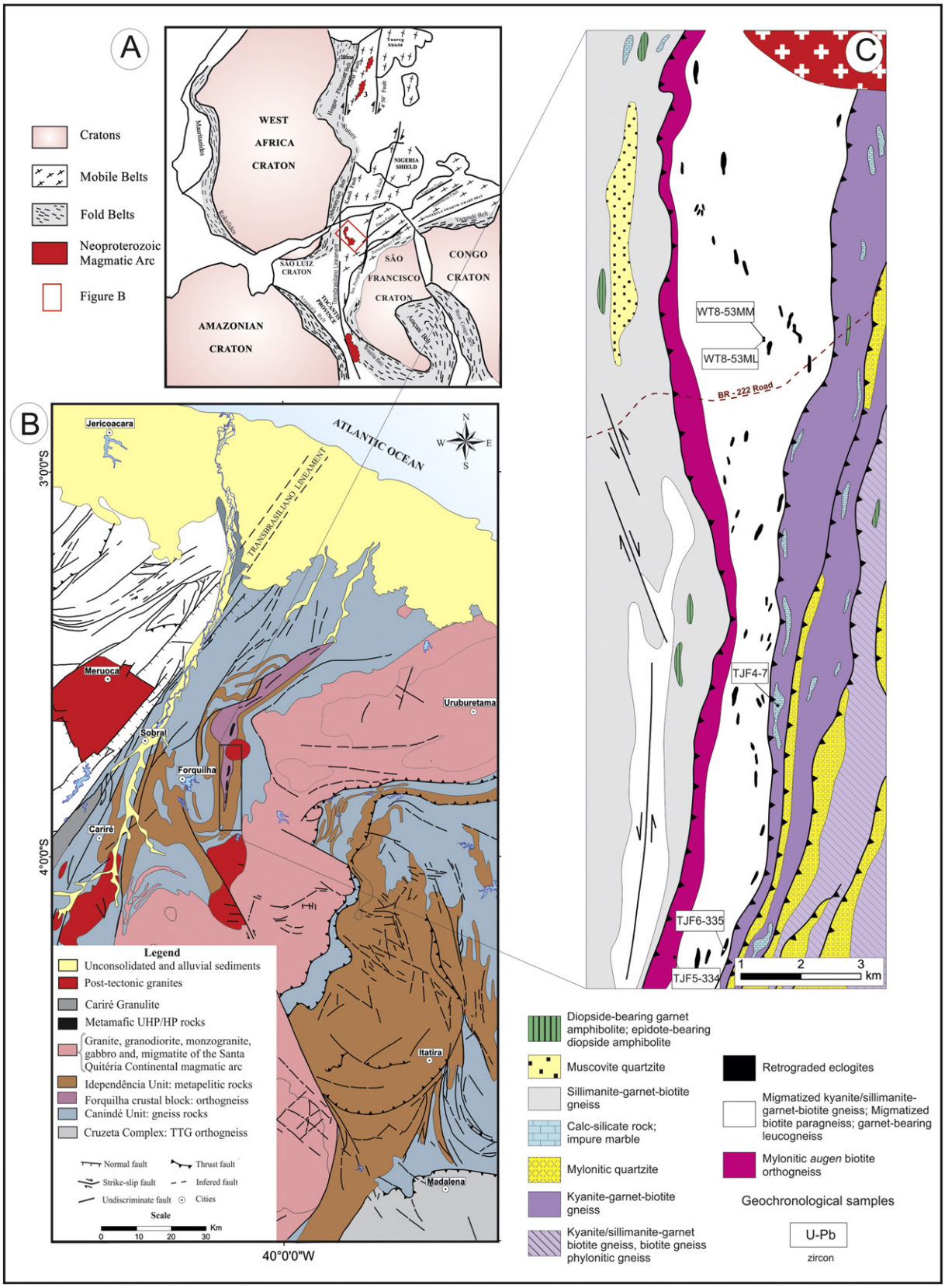

Fig. 1. Geologic setting of the study area. (A) Gondwana assembly during the Late Neoproterozoic; (B) NW portion of the Borborema Province showing the Santa Quitéria continental magmatic arc and the Transbrasiliano Lineament (modified after Cavalcante et al., 2003); (C) Detailed geological map of the FEZ (after Ancelmi et al., 2013).

Fuck, 1992; Pimentel et al., 2000; Valeriano et al., 2008) attest to subduction and ocean closure (Goianides Ocean). Based on the characterization of the Santa Quitéria continental magmatic arc (SQCMA) (Fig. 1B), Fetter et al. (2003) proposed the continuity of the Goianides Ocean northeastwards, into the Borborema Province. In addition to that, recent studies conducted by Santos et al. (2009b) and Amaral et al. (2011), involving

geochemical and thermobarometric data, have suggested that the metamafic rocks that occur between SQCMA and the Transbrasiliano lineament indicate a HP suture zone in the NW part of the Borborema Province, named Forquilha Eclogite Zone (FEZ; Fig. 1B). This zone is approximately 4 km wide and up to 30 km long and comprises mafic and ultramafic rocks represented by several varieties of clinopyroxene–garnet amphibolites and garnet amphibolites enclosed in migmatized quartz-feldspathic gneiss, sillimanite (after kyanite)-bearing paragneiss, and calc-silicate rocks. The mafic rocks occur as small, dismembered boudins, erratic blocks or sheets in the enclosing aluminous metasedimentary rocks and often in strongly sheared granodiorite gneiss (Fig. 1C).

For the first time, in this article we identify coesite by Raman microspectroscopy in combination with optical microscopy and scanning electron microscopy in an eclogite from the FEZ, NE Brazil and present U–Pb zircon ages for this UHP rock. Additionally, we obtained U–Pb monazite ages and zircon Hf isotope composition for host rocks of the eclogite, trying to determine the metamorphism timing related to the subduction and collisional event that occurred in the NW portion of the Province Borborema.

2. Geological setting

As indicated by geological and geochronological data (Fetter et al., 2000, 2003), the Transbrasiliano Lineament in the Borborema Province represents a major crustal-block boundary juxtaposing two crustal units: the Médio Coreaú and the Ceará Central domains (Fig. 1B), respectively on the east and west sides of the Transbrasiliano lineament.

The Médio Coreaú domain encloses a high-grade metamorphic basement complex composed mainly of orthogneiss with TTG affinity, amphibole gneiss, amphibolites, leucogranites, mafic granulite, enderbite, khondalite, kinzigite, and migmatite. U–Pb and Sm–Nd studies of these rocks established an Early Paleoproterozoic age (2.36–2.29 Ga) for the main gneisses, and yielded Nd crustal residence (T_{DM}) ages between 2.61 and 2.38 Ga, with positive (+0.5 to +1.9) εNd(t) values (at t = crystallization age) (Fetter et al., 2000; Santos et al., 2009a). This basement has been interpreted as representing juvenile crustal growth (Fetter et al., 2000), generated in an arc-type setting. A Late Paleoproterozoic (1.79 Ga) extensional event is represented by felsic to intermediate volcanic rocks, including trachyandesite, rhyodacite, rhyolite, volcanic breccias, and tuffs (Santos et al., 2008b).

Two main supracrustal sequences that unconformably overlie the basement of the Médio Coreaú domain are represented by Neoproterozoic metavolcano-sedimentary rocks (Santos et al., 2008b; Araújo et al., 2012). Four granite plutons intrude the Médio Coreaú domain. Two of them were affected and are related to the Brasiliano deformation and yielded crystallization ages between 590 and 560 Ma; the latter contemporary with the late transcurrent tectonic phase of the Brasiliano orogeny in the area (Santos et al., 2008b). The last two plutons are undeformed granites and represent post-orogenic intrusions (Fig. 1B), with crystallization age around 530 Ma (Santos et al., 2008b).

The Ceará Central domain is a crustal block composed of: (1) vast tracts of juvenile Middle Paleoproterozoic (2.14–2.10 Ga) high-grade felsic orthogneisses and migmatites with TTG affinity and slightly negative to positive $\varepsilon_{Nd\ (T\ =\ 2100\ Ma)}$, suggesting predominantly depleted mantle contribution with incipient crustal contamination (Fetter et al., 2000; Martins et al., 2009); (2) an inlier of Archean crust known as the Tróia-Pedra Branca massif with 2.75–3.27 Ga (da Silva et al., 2002), and (3) the roots of a Neoproterozoic continental arc known as the Santa Quitéria continental magmatic arc (Fetter et al., 2003; Arthaud et al., 2008) (Fig. 2). The supracrustal sequence of the Ceará Central domain is composed of metapelite, thick layers of quartzite and lenses of metalimestone and metamafic rocks affected by medium- to high-grade metamorphism, and represents a passive margin sequence deposited after 770 Ma (Arthaud et al., 2008).

In the southwestern portion of the Ceará Central domain the Novo Orient Group is exposed, represented by a Neoproterozoic metavolcano-sedimentary sequence. The metavolcanic unit comprises pillowed mafic and ultramafic rocks, interpreted as mantle slices or even as part of an oceanic crust with Nd model ages (T_{DM}) between 1.36 and 1.69 Ga (Araújo et al., 2010).

The Santa Quitéria continental magmatic arc (SQCMA) (Fetter et al., 2003) is a NE–SW trending complex of Brasiliano granitoid plutons and migmatites, covering around 40,000 km^2. U–Pb ages so far obtained for the complex range from 880 to 622 Ma (Fetter et al., 2003; Araújo et al., 2014). The Nd isotopic signatures are consistent with variable mixture of juvenile Neoproterozoic magmas and the surrounding Paleoproterozoic gneisses.

According to Santos et al. (2009b), the rock association bordering the western portion of the SQCMA comprises a sequence of biotite gneiss, sillimanite–garnet gneiss, muscovite–sillimanite quartzite, quartz–muscovite schist, amphibole gneiss, augen gneiss, garnet-bearing leucogranite and metamafic rocks. Based on detailed geological mapping (1:10,000) and petrography, Ancelmi et al. (2013) show that retrograded eclogite occurs enclosed in ortho- and para-gneiss and rarely in calc-silicate rocks, stretching out for more than 20 km and trending N–S to NE–SW (Fig. 1C). These rocks display a predominant low-angle, E-dipping foliation and low-medium angle (around 30°), E- or SE-plunging stretching lineation defined by sillimanite, quartz, biotite, and muscovite (Fig. 2A). The thrusting event evolves progressively to the strike–slip event to the west, represented by pervasive NE–SW to NS-trending and steeply dipping foliation with NE–SW to N–S subhorizontal stretching lineation. The mafic bodies occur as lenses and boudins, ranging from 0.5 to 100 m in width and 0.2 to 6 km in length (Fig. 2B), in different metamorphic grades, from eclogite (770 °C and 17.3 kbar), granulite (870 ± 40 °C and 14.5 ± 1.5 kbar), amphibolite (741 ± 93 °C and 12.2 ± 1.7 kbar), epidote amphibolite (595 ± 87 °C and 5.1 ± 1.3 kbar), to greenschist facies (460 ± 40 °C and 4.1 ± 1.0 kbar) (Santos et al., 2009b).

New U–Pb and Sm–Nd of metamafic rocks from the FEZ indicate crystallization ages between 1.5 and 1.6 Ga (Amaral et al., 2010; Amaral et al., in press). Likewise, provenance zircon U–Pb and Sm–Nd data of metasedimentary rocks that enclose the eclogitic rocks indicate Paleoproterozoic sources older than 1.85 Ga (Ancelmi et al., in review).

Our studies encompass a detailed petrographic analysis of the metamafic rocks, especially of the isotropic samples collected in the field. Around fifty bodies were mapped (Fig. 1C) and based on optical microscopy, backscattered scanning electron microscopy (BSE) and Raman micro-spectroscopy, UHP conditions were identified. U–Pb zircon and monazite and Lu–Hf zircon dating aimed at defining the timing of the metamorphic evolution of the FEZ. For this, six samples were dated: i) a mylonitic augen biotite orthogneiss in contact with FEZ; ii) a UHP metamafic rock; iii) a sillimanite gneiss, iv) leucosome and mesosome of a migmatite; v) a calc-silicate rock inside the FEZ, and vi) a tonalitic gneiss outcropping between the FEZ and the Transbrasiliano lineament.

3. Analytical procedures

Raman spectra of inclusions in garnet and clinopyroxene in thin sections were obtained at Institute of Geosciences—UNICAMP. The equipment is a laser-Raman multi-channel microprobe (CCD T64000 JOBIN-YVON) coupled with a high-resolution Olympus optical microscope (100×/0.80 objective) that focuses the laser radiation (Ar laser, line 514.5 nm excitation, 80 mW) on the sample (1 μm-diameter aperture and 3 μm-deep resolution). Each spectrum represents the accumulation of six acquisitions of 60 s to provide a good signal-to-noise ratio. The Raman frequencies were calibrated to 1 cm^{-1} using standard Ne emission lines. Raman mapping was recorded with a commercial Confocal Raman microscope (CRM 200-WiTec) of the Physics Institute-UNICAMP, Brazil. The laser radiation was coupled to the microscope via a single-mode fiber. The optical components (filters, gratings, and lenses) were adapted to the appropriate wavelength. The used Raman spectra were centered at $t_{coesite}$ 521 cm^{-1}. The following conditions were applied:

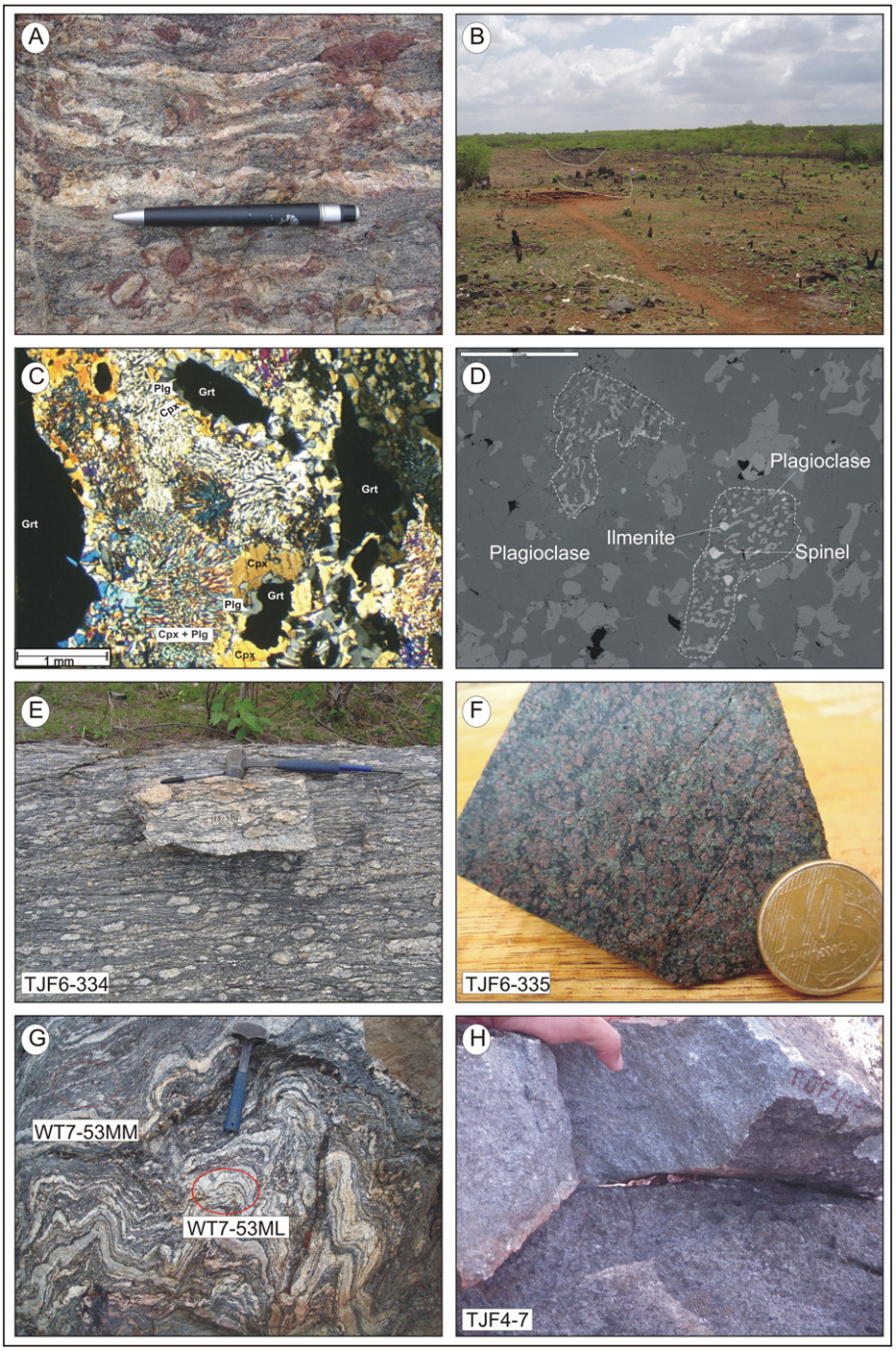

Fig. 2. Field and petrographic features of FEZ rocks. (A) Sillimanite garnet gneiss; (B) boudins of metamafic rocks; (C) Cpx + Pl symplectites replacing omphacite in sample (TJF6-355); (D) spinel + ilmenite + plagioclase symplectites in garnet pyroxenite; (E) FEZ basal mylonitic augen gneiss; (F) isotropic texture of coesite-bearing eclogite; (G) migmatized sillimanite-garnet gneiss, with indication of leucosome (WT7-53ML) and mesosome (WT7-53MM); (H) textural aspect of calc-silicate rock (sample TJF4-7).

integration time, 0.2 s (image) and 3 s (spectrum); objective used for Raman spectral 60× Nikon imaging, NA = 0.8 and excitation wavelength 633 nm. Spectra were treated with the Origin 6.1 and Witec project software.

U–Pb and Lu–Hf isotopic analyses were performed on zircon and monazite grains from six samples (Supplementary Tables 1–7), using a Thermo-Fisher Neptune MC-ICP-MS coupled with a Nd:YAG UP213 New Wave laser ablation system, installed in the Laboratory of Geochronology of the University of Brasilia—UnB.

The U–Pb analyses on zircon and monazite grains were carried out following Bühn et al. (2009). The laser was regulated with a spot size of 25–30 μm, at a frequency of 11 Hz and an intensity of approximately 0.8 J/cm^2. Normalization to GJ standard zircon (608.5 ± 1.5 Ma; Jackson et al., 2004) and the ages were plotted and calculated using the Isoplot 3.0 software (Ludwig, 2003). Corrections for common Pb were carried out in analyses presenting $^{206}Pb/^{204}Pb$ lower than 1000, using the Stacey and Kramers (1975) model at the age of crystallization. Frequency histograms were plotted according to the distribution of $^{207}Pb/^{206}Pb$ age with less than 10% discordance.

Lu–Hf isotopic analyses were performed following Matteini et al. (2010). The $\varepsilon Hf(t)$ values were calculated using the decay constant $\lambda = 1.865 * 10^{-11}$, proposed by Scherer et al. (2006), and the $^{176}Lu/^{177}Hf$ and $^{176}Hf/^{177}Hf$ CHUR values of 0.0332 and 0.282772, respectively, proposed by Blichert-Toft and Albarède (1997). The two-

stage depleted mantle Hf model ages (T_{DM} Hf) were calculated using $^{176}Lu/^{177}Hf = 0.0384$ and $^{176}Hf/^{177}Hf = 0.28325$ for the depleted mantle and $^{176}Lu/^{177}Hf$ of 0.0113 for the average crust (Chauvel and Blichert-Toft, 2001). During the analytical session, replicate analyses of GJ-1 standard zircon were carried out, resulting in a $^{176}Hf/^{177}Hf$ ratio of 0.282006 ± 16 2σ ($n = 25$), which agrees with the reference value for GJ standard zircon obtained by Morel et al. (2008).

4. Petrography and Raman results

The garnet–pyroxene amphibolite (TJF6-335) from the southern sector of the FEZ (UTM coordinates 371970; 9570622) occurs in boudins associated with marble, quartzite, calc-silicate rock, and kyanite–biotite schist (Fig. 1C). The boudin core, from which the sample was collected, is essentially isotropic and shows a dominant granoblastic texture characterized by garnet dispersed in a mesocratic matrix of plagioclase and clinopyroxene. Amphibole increases at boudin borders associated with mylonitic deformation. Thus, garnet clinopyroxenite is commonly surrounded by garnet–clinopyroxene amphibolite and garnet amphibolite. In a single outcrop different rock compositions are recognized as a function of fluid percolation along deformed zones.

The garnet clinopyroxenite from the core of boudins is a grayish-green rock composed of anhedral garnet porphyroblasts up to 3 mm in size, surrounded by less than 100 μm-thick, fine-grained plagioclase coronae. The matrix is composed of fine-grained clinopyroxene and plagioclase symplectite replacing omphacite in a decompression metamorphic phase (Fig. 2C). Occasionally, the preferred orientation of this symplectite texture suggests that it was formed during decompression conditions or this orientation corresponds to that of original omphacite. The most common symplectites are represented by clinopyroxene + plagioclase ± amphibole intergrowths, but other types of symplectites have also been observed, such as ilmenite + clinopyroxene, ilmenite + plagioclase, ilmenite + hematite, and corundum + spinel + ilmenite (Fig. 2D).

Around fifty bodies of metamafic rocks were individualized in the field, resulting in over two hundred thin sections. Under optical microscope we selected a number of samples based on amphibole-free composition, occurrence of clinopyroxene + plagioclase and atoll-type garnet crystals comprising complete or almost complete rim of garnet with a core filled by mineral inclusions. This type of structure, associated with HP conditions after overgrowth of UHP garnet (Arenas et al., 1997; Liu et al., 2006; Cheng et al., 2007), is present in sample TJF6-335 (Fig. 3A–B), and is an indirect evidence of eclogite facies conditions.

The corundum + garnet association in the coesite-bearing eclogite (sample TJF6-335A) may be taken as an additional UHP indicator (Morishita et al., 2001; Shimpo et al., 2006), as corundum exsolution corresponds to a high-pressure phase in garnet. The plagioclase–spinel–ilmenite symplectite could represent sapphire pseudomorph, which is a typical ultra-high temperature mineral phase, and be associated with a short event of high-temperature metamorphism after higher pressure peak metamorphism.

Coesite included in garnet, zircon, or clinopyroxene is an undisputed evidence of UHP metamorphism, but its characterization by optical microscope is indirect. Former coesite presence is recognizable by three features associated with its transformation to quartz: palisade quartz textures, polycrystalline quartz pseudomorphs and radial crack patterns around quartz inclusions. As a typical UHP mineral, coesite is normally not preserved in the rock due to retrograde metamorphism, but it can be quite common as inclusions in garnet, omphacite or zircon (Schreyer, 1995; Chopin, 2003; O'Brien and Ziemann, 2008). In two samples of garnet clinopyroxenite from the FEZ we identified radial fractures around quartz inclusions in clinopyroxene (Fig. 3C) and garnet (Fig. 3D), resulting from the volume change during the polymorphic coesite-to-quartz transformation.

The optically undetected coesite relicts were initially inferred by backscattered electron (BSE) imagery in several samples for subsequent Raman microspectroscopy study. In the atoll-type garnet we identified a quartz inclusion in its border with approximately 30 μm that displays two small, rounded, preserved grains of coesite with 2 to 3 μm diameter (Fig. 3E). Coesite and α-quartz are distinguishable in sample TJF6-335 by their diagnostic Raman spectra, where coesite displays a characteristic 521 cm^{-1} band, while quartz shows a strong 464 cm^{-1} band, with other weaker bands at 206, 265, 355, 394, 696, and 796 cm^{-1} (Fig. 3D). The diagnostic 521 cm^{-1} band of coesite in sample TJF6-335 displays moderate intensity (Fig. 3F), probably due to the size of the coesite grains, which were smaller than the laser beam and may have affected the Raman diffraction or due to sub-microscopic coesite grains in the transformed quartz (Ghiribelli et al., 2002; Zhang et al., 2005; Lu et al., 2008). To enhance the coesite characterization Raman mapping was conducted with a Confocal Raman Microscope CRM 200-Witec. The Raman spectrum was performed at 30 × 30 μm^2 in the sample in order to individualize the 521 peak. Thus, Raman mapping technique revealed two new unexposed coesite inclusions (Fig. 3G) that are unequivocal evidence of UHP conditions in the FEZ.

5. Geochronology

The coesite-bearing eclogite (sample TJF6-335 — a garnet clinopyroxenite) contains two zircon populations, one represented by elongated (3:1), euhedral to subhedral crystals, and the other by well rounded grains (Fig. 4C). The internal zircon textures by cathodoluminescence images illustrate well defined overgrowths and complex structures in both populations. In general, the spots were preferentially targeted in the center of the zircon grains. Forty-six zircon grains were analyzed, of which nineteen show higher than 90% concordance (Supplementary Table 1). Independently from the crystal morphology, all zircon grains display a Neoproterozoic age (Fig. 4A). Nine crystals yielded values close to 100% concordance, defining a concordia age of 614.9 ± 7.9 Ma (2σ) (Fig. 4B). Th/U ratio in zircon has been used to distinguish between magmatic (>0.1) and metamorphic (<0.1) origins (Rubatto, 2002), however this relationship is problematic, particularly in high grade rocks where the concentrations of Th and U in zircon are influenced by co-existing minerals (monazite, allanite), melts and fluids (Harley et al., 2007, and references therein). The garnet clinopyroxenite (TJF6-335) displays Th/U ratios between 0.01 and 0.53 (Supplementary Table 1), where the <0.1 values show $^{206}Pb/^{238}U$ ages between 816 and 633 Ma, while Th/U > 0.1 values display $^{206}Pb/^{238}U$ ages between 795 and 598 Ma.

The garnet clinopyroxenite (TJF6-335) overlies a N–S mylonitic biotite augen orthogneiss with 140/20 stretching-lineation (Figs. 1C and 2E). The augen gneiss (Sample TJF6-334) displays a U–Pb zircon age of 2092 ± 17 Ma (Fig. 4D) (Supplementary Table 2) considered as its crystallization age. A tonalite gneiss to the west of the FEZ (Sample TJF6-317) displays crystallization U–Pb zircon age of 2021.4 ± 8.1 Ma (Fig. 4E) (Supplementary Table 3). Both rocks and the paragneisses constitute a Paleoproterozoic crustal block between the Santa Quitéria continental magmatic arc and the Transbrasiliano lineament.

The metamafic rocks from the central portion of the eclogitic belt are enclosed in migmatized sillimanite–garnet–biotite gneiss, kyanite–garnet–biotite gneiss and garnet-bearing biotite gneiss. An imbricated migmatitic kinzigite (UTM 373378/9580594) composed of sillimanite (after kyanite) + garnet + biotite + alkali-feldspar + rutile ± plagioclase, strikes parallel to the regional tectonic framework, dipping eastwards at low angles. Thermobarometric studies in this rock indicate minimum P–T conditions at around 12 kbar and 825 °C (Santos et al., 2009b). Furthermore, portions of this sequence experienced a great degree of migmatization, leading to the formation of anatectic rocks represented by sillimanite-garnet leucogranites. The mesosome of migmatite is constituted of centimeter-sized garnet, biotite and plagioclase. The leucosome comprises dominantly millimeter-sized garnet, plagioclase, quartz, K-feldspar, kyanite and sillimanite mantled by garnet. Aiming at a better definition of both zircon provenance and timing of the migmatization event, both zircon and monazite from the mesosome

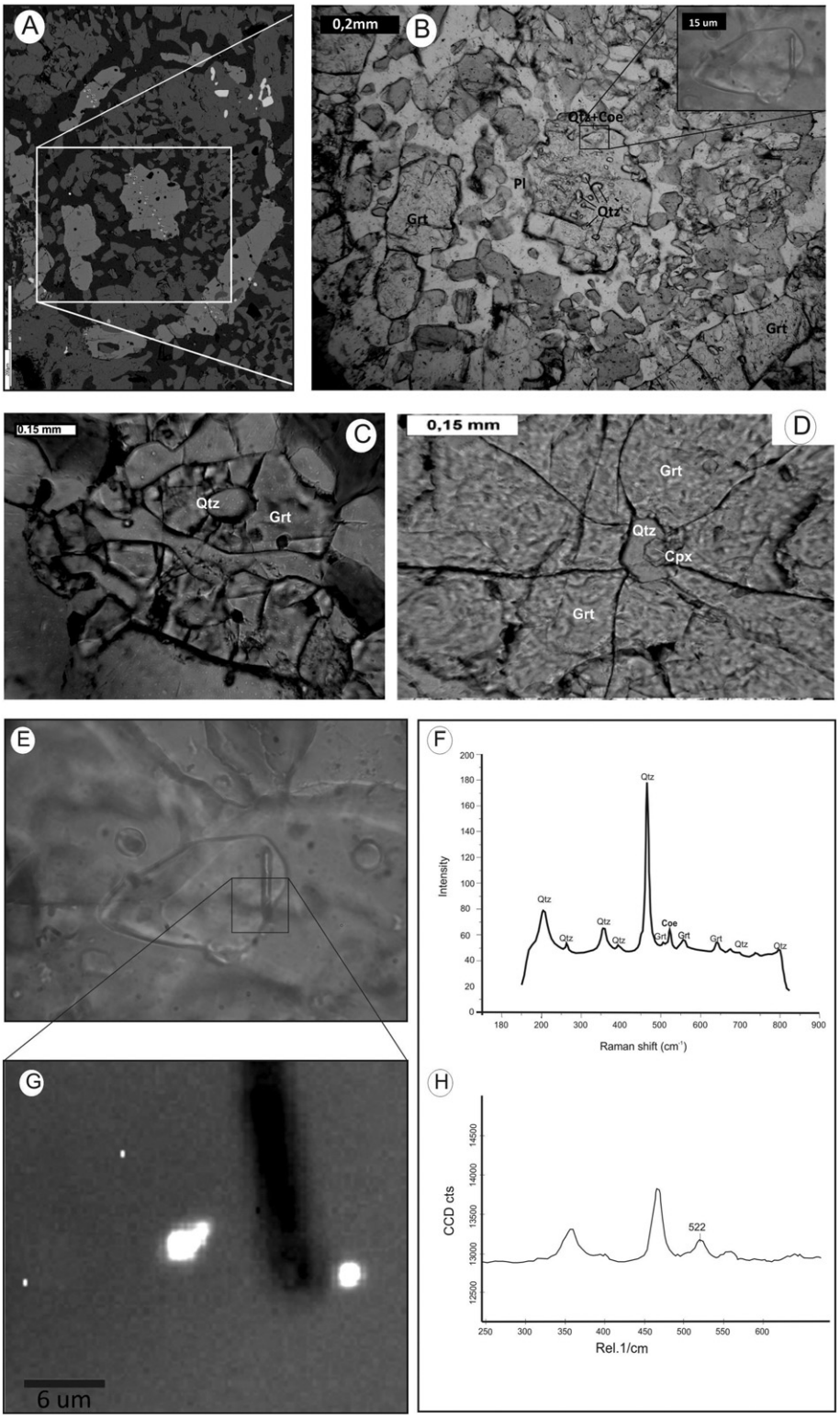

Fig. 3. Microtextural features and Raman spectroscopy of coesite-bearing eclogite. (A) Backscattered electron image of atoll-type garnet crystals; (B) Photomicrography of atoll-type garnet with quartz inclusions in its border with small grains of coesite; (C) garnet (Grt) showing radial fractures around retrograde quartz (Qtz) inclusion (sample TJF6–335); (D) radial fracture around quartz (Qtz) included in garnet (Grt) (garnet pyroxenite, sample WT7-25 K); (E) detail of quartz with coesite relics and rutile inclusion; (F) Raman spectra where coesite displays a characteristic 521 cm^{-1} band, while quartz shows a strong 464 cm^{-1} band and other weaker bands; (G) Raman mapping of quartz (gray) showing coesite relics (white) and rutile (black) inclusion; (H) Raman spectrum of the coesite core.

(sample WT8-53MM) and leucosome (sample WT8-53ML) (Fig. 2G) have been analyzed. The mesosome zircon grains were grouped into two families. Crystals of the first family are rounded and ca. 100 μm in size, usually transparent, and contain few inclusions and fractures (Z5, Z9, and Z10 in Fig. 5C). Well-defined oscillatory zoning is characteristic of the cores and the grains are enveloped by a later overgrowth. The second family is composed of yellowish, elongated grains, in the average 200-μm long, and usually euhedral with prismatic faces. Backscattered

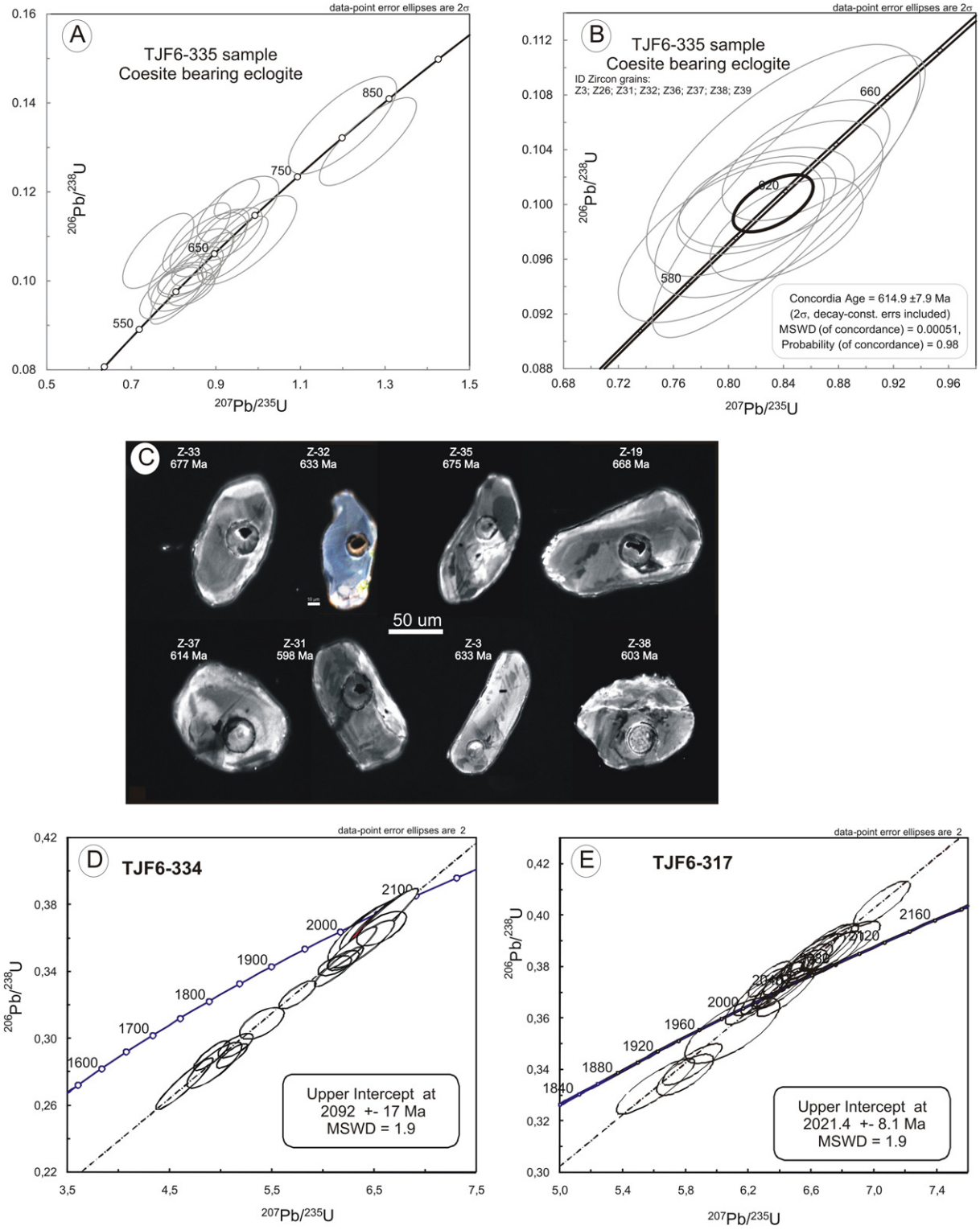

Fig. 4. LA-ICP-MS U–Pb analyses and textural features of zircon of sample TJF6-335. (A) Concordia diagram showing all data; (B) concordant zircon age of 614.9 ± 7.9 Ma correspondent to the retrograde metamorphic time; (C) cathodoluminescence image (CL) of zircon from coesite-bearing eclogite showing homogeneous and diffuse texture with variable morphology (ratio 3:1 to 1:1); (D) U–Pb concordia diagram for mylonitic augen gneiss (sample TJF6-334) with a crystallization age of 2092 ± 17 Ma; (E) U–Pb concordia diagram for tonalitic gneiss (sample TJF6-317) with a crystallization age of 2021.4 ± 8.1 Ma.

electron images illustrate both metamictization along internal structures and a well-defined oscillatory zoning (Z21, Z13, Z14 in Fig. 5C). Most crystals are devoid of fractures.

Leucosome sample WT8-53ML also displays two zircon families. One family encompasses light brownish, slightly elongated, subhedral grains, which may preserve some intact crystal faces (Z10 and Z12 in Fig. 5E). Zircon cores are enveloped by a thin, intergrowth oscillatory layer and show some degree of metamictization. The second family comprises grains of ca. 100 to 150 μm in size, pink to colorless, subhedral or with partially rounded faces. Internal structures are marked by concentric oscillatory zoning. Backscattered electron images show that some zircon grains present metamorphic overgrowths (Z11 and Z14

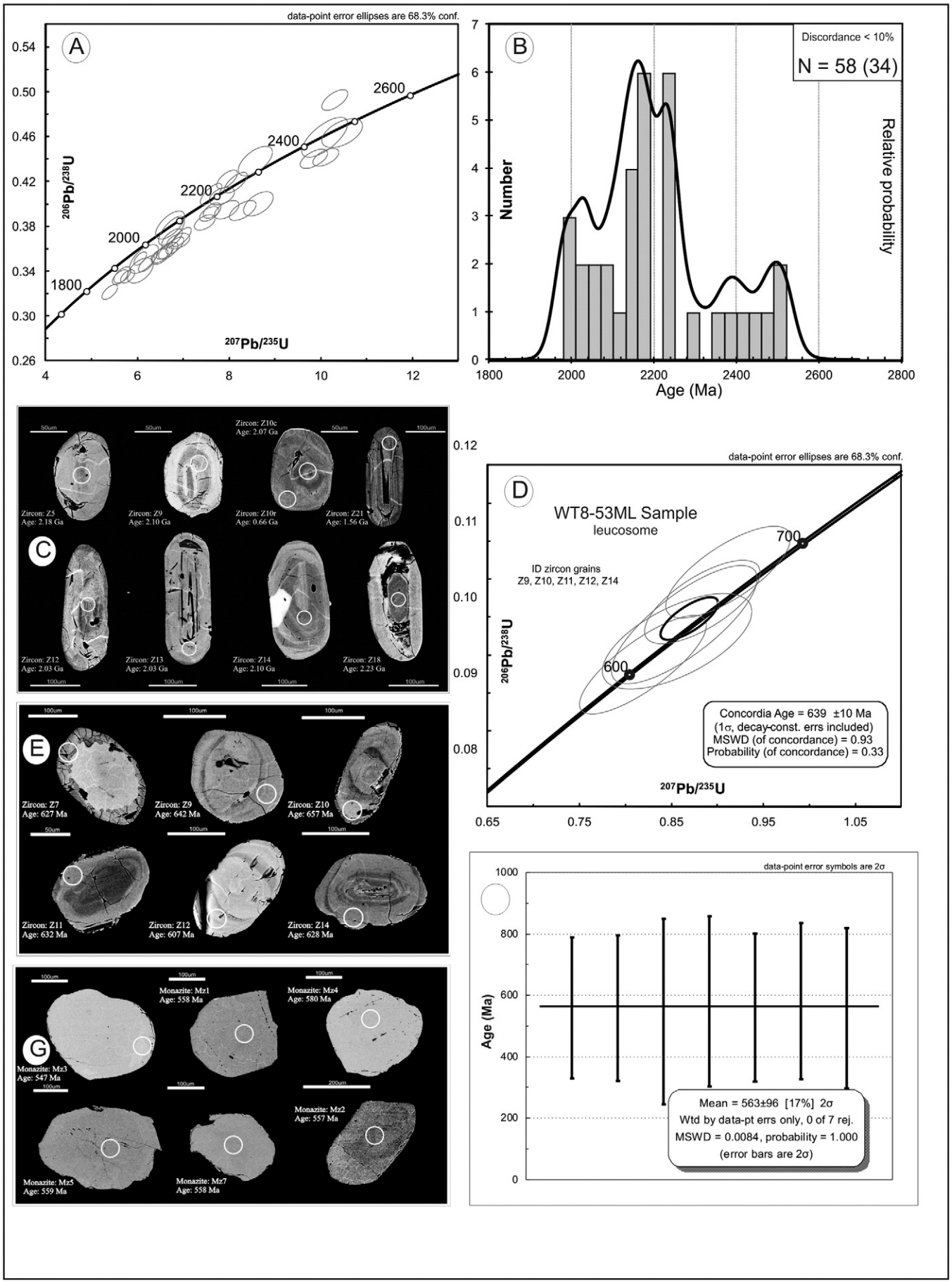
data-point error ellipses are 68.3% conf.
A
$^{206}Pb/^{238}U$
$^{207}Pb/^{235}U$
1800
2000
2200
2400
2600
B
Discordance < 10%
N = 58 (34)
Number
Relative probability
Age (Ma)
C
Zircon: Z5 Age: 2.18 Ga
Zircon: Z9 Age: 2.10 Ga
Zircon: Z10c Age: 2.07 Ga
Zircon: Z10r Age: 0.66 Ga
Zircon: Z21 Age: 1.56 Ga
Zircon: Z12 Age: 2.03 Ga
Zircon: Z13 Age: 2.03 Ga
Zircon: Z14 Age: 2.10 Ga
Zircon: Z18 Age: 2.23 Ga
D
data-point error ellipses are 68.3% conf.
WT8-53ML Sample
leucosome
ID zircon grains
Z9, Z10, Z11, Z12, Z14
700
600
Concordia Age = 639 ±10 Ma
(1σ, decay-const. errs included)
MSWD (of concordance) = 0.93
Probability (of concordance) = 0.33
E
Zircon: Z7 Age: 627 Ma
Zircon: Z9 Age: 642 Ma
Zircon: Z10 Age: 657 Ma
Zircon: Z11 Age: 632 Ma
Zircon: Z12 Age: 607 Ma
Zircon: Z14 Age: 628 Ma
G
Monazite: Mz1 Age: 558 Ma
Monazite: Mz4 Age: 580 Ma
Monazite: Mz3 Age: 547 Ma
Monazite: Mz2 Age: 557 Ma
Monazite: Mz5 Age: 559 Ma
Monazite: Mz7 Age: 558 Ma
data-point error symbols are 2σ
Age (Ma)
Mean = 563±96 [17%] 2σ
Wtd by data-pt errs only, 0 of 7 rej.
MSWD = 0.0084, probability = 1.000
(error bars are 2σ)

in Fig. 5E). The monazite grains are relatively uniform, sub-rounded, yellowish to orange, and devoid of inclusions or fractures (Fig. 5G).

The age distribution in the concordia diagram (Fig. 5A) and the frequency histogram (Fig. 5B) showing all data (Supplementary Table 4) obtained for zircon crystals from the migmatite mesosome (sample WT8-53MM) clearly indicates a predominant source between 2.0 and 2.2 Ga. Archean ages of ca. 3.0 Ga are interpreted as resulting from higher metamictization intensities that affected some grains. Only one crystal recorded ages close to 1.57 Ga. The other grains yielded ages distributed in the 1.9 and 2.5 Ga interval (Fig. 5A–B).

The data obtained for zircon grains from the migmatite leucosome (sample WT8-53ML) (Supplementary Table 5) define an age of 639 ± 10 Ma (2σ) in the concordia diagram, interpreted as the metamorphic migmatization record (granulite facies?) (Fig. 5D). For monazite, weighted mean $^{235}U/^{207}Pb$ ratios yielded a mean age of 563 ± 96 Ma (2σ) (Fig. 5F). Considering the physical–chemical conditions for monazite crystallization at temperatures lower than those for zircon, the age obtained can be interpreted as the record of low-grade metamorphic conditions or even retrograde metamorphism (lower amphibolite facies), although the accuracy of this is an open question.

Lenses of calc-silicate rock occur associated with retrogressed eclogite from the southern sector (Fig. 1C). The outcrops are varied in size, exceeding 50 m × 30 m. The calc-silicate rocks are olive green and medium- to coarse-grained, with biotite (30%), amphibole (15%), pyroxene (25%), plagioclase (15%), quartz (10%) and garnet (5%). These rocks are imbricated with aluminous paragneisses dipping 30° E–SE and characterized by a down-dip biotite lineation.

Fifty-one grains that compose two zircon families extracted from a calc-silicate rock (sample TJF4-7 — UTM 373072; 9576482) were analyzed (Supplementary Table 6). In one family the grains are yellowish, sub-rounded to rounded (2:1) (Z24, Z47 and Z56 in Fig. 6E) or prismatic (3:1) (Z41 and Z53 in Fig. 6E), and show oscillatory zoning. Metamictization is evidenced by the presence of fractures at crystal rims (Z43, Z53 and Z56). The explanation for this is that the zircon core is richer in U than the rim and the expansion of the core during metamictization caused fracturing of the more rigid rim (Corfu et al., 2003). The zircon crystals of the other family are transparent and either rounded (1:1) (Z2 and Z3 in Fig. 6E) or elongated, with sub-rounded to rounded terminations (Z15 and Z33 Fig. 6E) (3:1). Neither internal structures nor evidence of metamictization are recognized in the backscattered electron images. The data from the cores of the 51 zircon grains are represented in the concordia diagram and a frequency histogram, which shows at least two populations: one in the 640 and 700 Ma range and another in the 2000 and 2250 Ma interval (Fig. 6A, B). The crystals showing around 100% concordance yielded ages of 660 ± 4 Ma (Fig. 6C) and 646 ± 4 Ma (Fig. 6D).

Model ages from the calc-silicate rock (sample TJF4-7) obtained by the Lu–Hf method applied to the same zircon grains analyzed by the U–Pb method yielded ca. 650 Ma for concordant zircon grains and 2100 Ma for the Paleoproterozoic grains (Supplementary Table 7). The former yielded T_{DM} values between 2.44 and 2.62 Ga with negative εHf values (t = 650 Ma) varying between –1.9 and –21, whereas the latter yielded T_{DM} between 1.9 and 2.45 Ga with positive εHf values (t = 2100 Ma) varying between +1.4 and +11 (Fig. 6F).

6. Discussion

The peak metamorphic condition is defined by coesite inclusions in garnet and clinopyroxene. The presence of coesite is characterized by typical radial fractures in garnet and principally, by Raman spectrum and Raman mapping technique, which led to the identification of four grains. The retrograde conditions of UHP rocks were presented by Santos et al. (2009b), which are represented initially by Na-rich clinopyroxene + pyrope-rich garnet + rutile + quartz that indicate 770 °C and 17.8 kbar. The retrograde stage in the granulite field is represented by the generation of plagioclase + augite coronae around garnet and plagioclase + augite symplectites after Na-rich clinopyroxene at 870 ± 40 °C for 14.5 ± 1.5 kbar. The amphibolite stage is marked by the formation of mainly small amphibole crystals around clinopyroxene + plagioclase symplectites and around garnet coronae formed of plagioclase, possibly by partial hydration of the previous assemblage. Replacement of rutile and/or ilmenite by titanite occurred probably in this stage. The epidote amphibolite stage is characterized by formation of titanite coronae around ilmenite and the transformation of andesine to oligoclase at 595 ± 87 °C and 5.1 ± 1.3 kbar. The final retrograde to greenschist stage was reported locally as the formation of Mg-rich chlorite and biotite after garnet along fractures and by the replacement of calcic hornblende by actinolite along borders and cleavage planes, estimated at 460 ± 40 °C and 4.1 ± 1.0 kbar (Santos et al., 2009b).

The metamafic rocks from the FEZ yielded a crystallization age around 1.5–1.6 Ga (Amaral et al., 2010; Amaral et al., in press) and were positioned as dykes or sills (Fig. 7A) in a Paleoproterozoic terrain (2.0–2.1 Ga) composed of mylonitic granite orthogneiss, tonalite gneiss, and metasedimentary rocks. Provenance study by U–Pb and Sm–Nd of these metasedimentary rocks shows exclusive Paleoproterozoic sources, older than 1.85 Ga (Ancelmi et al., in review).

The coesite-bearing eclogite (sample TJF6-335) records a zircon population with slightly rounded and clean grains less than 100 μm in size that are typical of high-temperature granulites (Corfu et al., 2003). Most of them are concordant and overlap concordia with good analytical agreement, defining an age of 614.9 ± 7.9 Ma. The zircon grains are dominantly rounded, and rarely preserve euhedral faces, and the internal texture is very complex, showing irregular zoning with diverse internal zoning-patterns in cathodoluminescence images, which suggests rocks subjected to HP-UHP conditions (Fig. 4) (Rubatto and Gebauer, 2000). The retrograde eclogite from the FEZ dated by the U–Pb zircon SHRIMP displays similar results (616 ± 4 and 625 ± 8.5 Ma) with commonly low Th/U (mostly 0.01–0.05) and no significant Eu-anomaly (Araújo, 2014). Generally, coesite is preserved only in rocks that underwent very fast exhumation. So far, diamond has not been reported in the study area; thus, it is proposed that the metamorphic peak pressure of the HP–UHP FEZ was lower than those of the diamond stability field ($28 < P < 35$ kbar). Thermobarometric calculation for the eclogite facies conditions defines temperature around 770 °C (Santos et al., 2009b), which indicates that the metamafic and metasedimentary rocks of the FEZ have been subducted to depths exceeding 90 km and were exhumed as fast extrusive slices pushed up above a low-angle thrust. Although more detailed thermobarometric studies are needed, and considering the errors in ages and making assumptions about the conversion of pressure to depth, it is possible to estimate a range of exhumation rates from 1.63 to 12.5 mm/yr.

U–Pb zircon metamorphic ages for two metasedimentary rocks, a sillimanite gneiss (WT8-53 ML) and a calc-silicate rock (TJF4-7) display concordant ages of 639 ± 10 Ma and 649.7 ± 5 Ma, respectively. The crystals that yielded these ages underwent metamorphism. Zircon grains from the sillimanite gneiss present internal igneous core and a

Fig. 5. LA-MC-ICP-MS U–Pb diagrams and textural features of zircon and monazite grains of migmatized garnet–sillimanite gneiss (samples WT8-53MM and WT8-53ML). (A) U–Pb concordia diagram for migmatite mesosome (sample WT8-53 MM); (B) Histogram of U–Pb ages for migmatite mesosome (discordance < 10%); (C) Backscattered electron images of representative mesosome zircon crystals. Inset: spots analyzed by the U–Pb method (spot size = 30 μm) and corresponding $^{235}U/^{207}Pb$ age; (D) U–Pb concordia diagram for migmatite leucosome (sample WT8-53 ML); (E) Backscattered electron images of representative zircon crystals from sample WT8-53ML leucosome. Two populations were identified: elongated grains (Z10 and Z12) and ovoid and rounded grains (Z7, Z9, Z11 and Z14). Inset: spots analyzed by the U–Pb method (spot size–25 μm), mostly grain rims, with corresponding $^{235}U/^{207}Pb$ ages; (F) frequency histogram for the U–Pb analyses of mesosome zircon (sample WT8-53MM); (G) backscattered electron images of representative monazite crystals from sample WT8-53ML leucosome. Inset: spots analyzed by the U–Pb method (spot size = 30 μm) with corresponding $^{235}U/^{207}Pb$ ages.

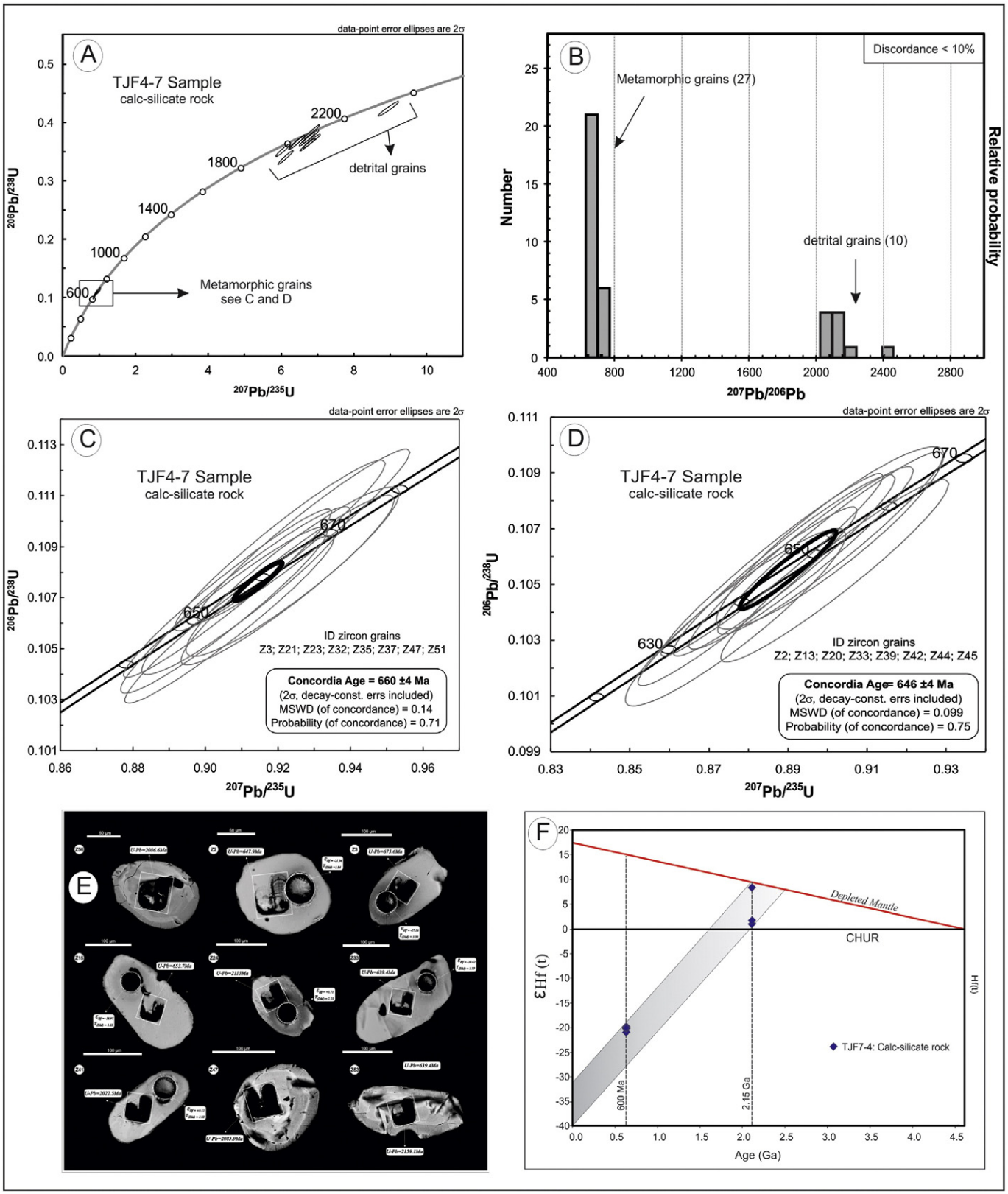

Fig. 6. U–Pb and Lu–Hf diagrams for zircon grains from calc-silicate rock of the FEZ. (A) Concordia diagram for U–Pb analyses (LA-MC-ICP-MS); (B) frequency histogram for zircon U–Pb ages of sample TJF4–7; (C–D) concordia diagram showing the metamorphic ages of U–Pb analyses (LA-ICPMS) of sample TJF4–7; (E) backscattered electron images of representative zircon crystals from sample TJF4–7. Inset: spots analyzed by the U–Pb (raster) and Lu–Hf (spot size = 30 μm) methods with corresponding $^{235}U/^{207}Pb$ ages, T_{DM} Hf and ε_{Hf} values; (F) evolution diagram showing ε_{Hf} values calculated for 2150 and 600 Ma.

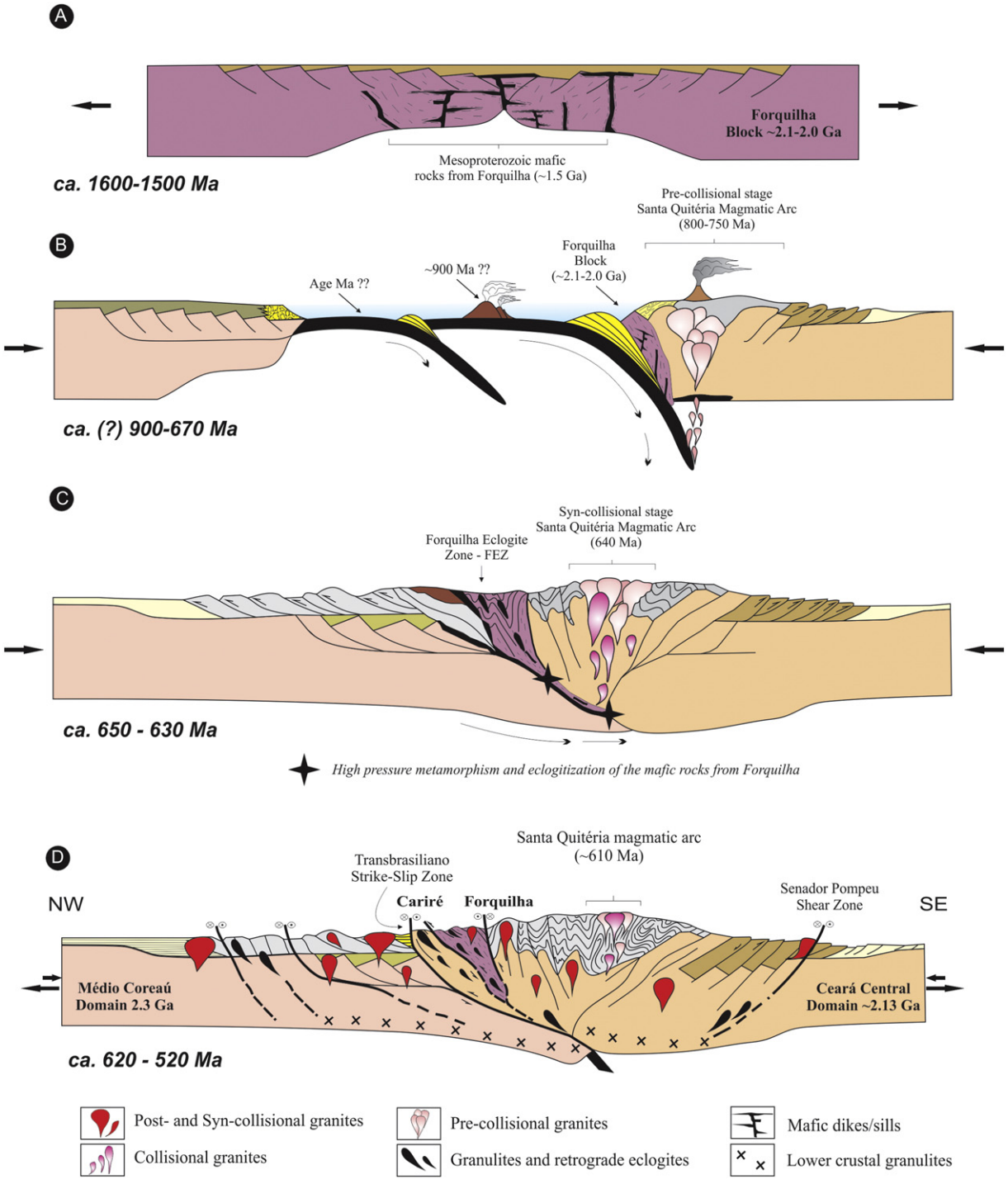

Fig. 7. Sketch tectonic model (*modified from* Van Der Pluijm and Marshak, 1997) showing the geodynamic evolution for the northwest portion of the Ceará Central domain. (A) Rifting of Paleoproterozoic crustal block (2.0–2.1 Ga); (B) early convergence with development of intra-oceanic arc (around 900 Ma?) and initial stage of the continental-arc magmatism (>700 Ma); (C) collisional stage with a closure of an oceanic realm and uplift of HP-UHP rocks of the FEZ; (D) final stage of the Santa Quitéria magmatism (around 610 Ma), emplacement of transtensional granite (around 570 Ma) and post-tectonic granites (<520 Ma) (modified from Van Der Pluijm and Marshak, 1997).

well-defined overgrowth rim. Two well-defined zircon populations were extracted from the calc-silicate rock, one yielding ages of ca. 2.1 Ga and the other of ca. 0.64 Ga. Model ages obtained by the Lu–Hf method and carried out in the same crystals analyzed by the U–Pb method were calculated for the Neoproterozoic (ca. 650 Ma) and Paleoproterozoic concordant zircon grains. For the former T_{DM} between 2.44 and 2.62 Ga and negative εHf values (t = 650 Ma) varying between −18 and −21 were obtained. The Paleoproterozoic zircon grains define T_{DM} values between 1.92 and 2.45 Ga and positive εHf values (t = 2100 Ma), varying between +1.4 and +11. The Hf isotopic compositions are approximately the same of the parental magma from which zircon crystallized, as indicated by the high Hf concentrations in this mineral (Blichert-Toft et al., 1997; Andersen et al., 2002; Griffin et al., 2002). The Lu–Hf data obtained for these Neoproterozoic zircon crystals indicate a Paleoproterozoic mantle derivation (~2.44 Ga) and highly negative ε_{Hf} values when calculated for 650 Ma. Therefore, it is evident

that the zircon crystals that yielded these ages were re-equilibrated during the Neoproterozoic metamorphic event. In any case, the 649.7 ± 5 Ma age is the oldest obtained for the Ceará Central domain high-grade metamorphism.

Subduction of oceanic lithosphere during the Neoproterozoic originated the Santa Quitéria Magmatic arc (Fetter et al., 2003). Based on SHRIMP U–Pb dating and Hf–O isotope analyses of zircon, Araújo et al. (2014) define three main evolution stages: early juvenile arc magmatism at ca. 880–650 Ma, mature Andean-type arc magmatism at ca. 660–630 Ma and crustal anatexis at 625 Ma until 600 Ma (Fig. 7B–C).

The 614.9 ± 7.9 Ma age, obtained for concordant zircon grains, is interpreted as record of the minimum age of the medium- to high-grade metamorphic conditions (upper amphibolite/granulite facies), and mainly characterized in the metamafic rocks. Several U–Pb analyses of zircon and monazite from deformed igneous rocks of the northwestern portion of the Ceará Central domain indicate that tangential collision took place after 620 Ma, and the transition to transcurrent tectonism occurred ca. 600 Ma (Santos et al., 2008b; Arthaud et al., 2008; Araújo et al., 2012). Likewise, the detailed study of metamorphic overgrowths in zircon grains (Garcia et al., 2014) defines the regional high-grade metamorphism around 620–630 Ma, an age also supported by Sm–Nd mineral–whole-rock isochron (621 ± 13 Ma). Similarly, based on U–Pb monazite data from aluminous migmatite gneiss of the Ceará Central domain, Castro (2004) defines the range of 640–630 Ma for the high-grade metamorphism (Fig. 7C).

During the transcurrent tectonic regime, several granite plutons were emplaced in transtractive belts (Fetter, 1999; Santos et al., 2008b) around 575 Ma (Fig. 7D). Mica and amphibole cooling ages ($^{40}Ar/^{39}Ar$) obtained by Monié et al. (1997) suggest that the transcurrent movements should have continued up to 540 Ma. 600–560 Ma comprises a still imprecise time interval defined by zircon and monazite. However, several authors have attributed this period to the installation of major shear zones in the Ceará Central and Médio Coreaú domains (Monié et al., 1997; Fetter et al., 2003; Archanjo et al., 2013; Viegas et al., 2014). In the Cariré region, rounded concordant zircon grains extracted from high-pressure mafic granulites and the rims of zircon grains from a host granodiorite from the same region yielded ages of 589 ± 8.9 Ma and 587 ± 31 Ma, respectively (Amaral et al., 2012). These data were interpreted as the record of high-grade metamorphism in this region. Nogueira Neto et al. (1997) obtained an age around 560 Ma for titanite from the Cariré mafic granulites, which is interpreted as that of the amphibolite facies metamorphic event associated with the development of a fault system that composes the Transbrasiliano Lineament. The final tectonic evolution is marked by the post-orogenic granites (Serra do Barriga, Mucambo, and Meruoca) around 530 Ma (Santos et al., 2008b).

Ocean crust and its subduction during the Late Neoproterozoic are properly documented in the Pharusian belt by the occurrence of HP-UHP terrains and calc-alkaline magmatism (Agbossoumondé et al., 2001; Caby, 2003; Agbossoumondé et al., 2004; Attoh and Morgan, 2004; Caby et al., 2008) and isotopic evidence of juvenile material in Central Brazil (Pimentel et al., 1991; Pimentel and Fuck, 1992; Pimentel et al., 2011). The junction between the Goianides and Pharusian Ocean has been approached in several papers, the Borborema Province being an important link for the correlation (Caby, 1989; Castaing et al., 1994; Trompette, 1994; Fetter et al., 2003; Santos et al., 2008a, 2009a). Uncontested Neoproterozoic suture zones are well defined in Africa, mainly by the occurrence of HP and UHP mafic and ultramafic rocks (Caby, 2003 and references therein).

7. Conclusion

High-pressure metamorphic conditions in the NW Borborema Province have been recognized in the FEZ (Santos et al., 2009b) and the Cariré region (Amaral et al., 2012), despite the lack of direct evidence, mainly due to the intense retrograde metamorphism recorded after the Brasiliano/Pan-African tectonic collage. The coesite inclusions in garnet grains from a garnet pyroxenite (sample TJF6-335) are a direct and indisputable evidence for UHP metamorphism of eclogite facies, suggesting deep subduction of the edge of the continental Forquilha block, probably related by slab pull from the descending oceanic lithosphere (Fig. 7).

The identification of an UHP metamorphic event in the northwestern portion of the Borborema Province, between the Santa Quitéria continental magmatic arc and the Transbrasiliano Lineament, which probably extends from Forquilha until Cariré–Novo Oriente and beyond, has important tectonic implications for the assembly of West Gondwana. The exact age of the UHP metamorphism is an open question, although regional high-grade metamorphism (amphibolite–granulite) displays a consistent age around 640 ± 10 Ma and the metamorphic eclogitic peak is older. It turns a transcontinental suture zone east of the Transbrasiliano lineament and its connection with the Brasília belt, in Central Brazil, an important feature (Fig. 7), which is covered by Paleozoic sedimentary rocks of the Parnaíba basin.

The occurrence of coesite in the garnet clinopyroxenite preserved in the core of boudins included in paragneiss is an evidence of continental lithosphere subduction. The characterization of Neoproterozoic oceanic crust in the Ceará Central domain remains uncertain, however the juvenile arc magmatism at least 880 Ma proves an intra-oceanic subduction (Araújo et al., 2014). The subduction duration remains uncertain; however the final stage with ocean closure and continental collision is marked by syn-collisional magmatism present in the Santa Quitéria continental magmatic arc around 640–650 Ma (Fig. 7) (Fetter et al., 2003; Araújo et al., 2012; Araújo et al., 2014).

Acknowledgments

The authors acknowledge the support of the Research Foundation of the State of São Paulo (FAPESP), Brazil (proc. 07/58.535-6), and the Brazilian National Research Council (CNPq) (INCT *Instituto Nacional de Ciência e Tecnologia em Estudos Tectônicos* — proc. 573713/2008-1). We would also like to thank Dailto Silva (Geosciences Institute) and Omar Tescke and Luiz Bonugli (Physics Institute of State University of Campinas — UNICAMP) for the access to Raman spectrometers and Erica M. Tonetto for her assistance with the cathodoluminescence images. TJSS, RAF and ELD acknowledge CNPq research fellowships. We gratefully acknowledge the critical and constructive reviews by Sérgio P. Neves and an anonymous reviewer and the associate editor Zeming Zhang for their comments and reviews.

Appendix A. Supplementary data

Supplementary data to this article can be found online at http://dx.doi.org/10.1016/j.gr.2014.09.013.

References

Affaton, P., Rahaman, M.A., Trompette, R., Sougy, J., 1991. The Dahomeyide Orogen: tectonothermal evolution and relationships with the Volta basin. In: Dallmeyer, D., Lécorché, J.P. (Eds.), The West African Orogens and Circum-Atlantic Correlatives. Springer, Berlim Heidelberg, pp. 107–122.

Agbossoumondé, Y., Ménot, R.P., Guillot, S., 2001. Metamorphic evolution of Neoproterozoic eclogites from south Togo (West Africa). Journal of African Earth Sciences 33, 227–244.

Agbossoumondé, Y., Guillot, S., Ménot, R.P., 2004. Pan-African subduction–collision event evidenced by high-P coronas in metanorites from the Agou massif (southern Togo). Precambrian Research 135, 1–21.

Amaral, W.S., Santos, T.J.S., Wernick, E., Matteini, M., Dantas, E.L., Moreto, C.P.N., 2010. U–Pb, Lu–Hf and Sm–Nd geochronology of rocks from the Forquilha Eclogite Zone, Ceará Central Domain, Borborema Province, NE—Brazil. VII SSAGI Abstracts. Brasília, pp. 113–116.

Amaral, W.S., Santos, T.J.S., Wernick, E., 2011. Occurrence and geochemistry of metamafic rocks from the Forquilha Eclogite Zone, Central Ceará (NE Brazil): geodynamic implications. Geological Journal 46, 137–155.

Amaral, W.S., Santos, T.J.S., Wernick, E., Nogueira Neto, J.A., Dantas, E.L., Matteini, M., 2012. High-pressure granulites from Cariré, Borborema Province, NE Brazil: tectonic setting, metamorphic conditions and U–Pb, Lu–Hf and Sm–Nd geochronology. Gondwana Research 22, 892–909. http://dx.doi.org/10.1016/j.gr.2012.02.011.

Amaral, W.S., Santos, T.J.S., Ancelmi, M.F., Fuck, R.A., Dantas, E.L., Matteini, M., Moreto, C.P. N., 2014. 1.57 Ga protolith age of the Neoproterozoic Forquilha eclogites, Borborema Province, NE-Brazil, constrained by U-Pb, Hf and Nd isotopes. Journal of South American Earth Sciences (in press).

Ancelmi, M.F., Santos, T.J.S., Reginato, R.A., Amaral, W.S., Monteiro, L.V.S., 2013. Geologia da Faixa eclogítica de Forquilha, Domínio Ceará Central, NW da Província Borborema. Brazilian Journal of Geology 43, 235–252.

Ancelmi, M.F., Santos, T.J.S., Amaral, W.S., Dantas, E.L., 2014w. Provenance of metasedimentary country rocks of retrograded eclogites from FEZ based on detrital U–Pb zircon ages and Nd isotopic data, NW Borborema Province, Brazil. Journal of South American Earth Sciences (in review).

Andersen, T., Griffin, W.L., Pearson, N.J., 2002. Crustal evolution in the SW part of the baltic shield: the Hf isotope evidence. Journal of Petrology 43, 1725–1747.

Araújo, C.E.G., Pinéo, T.R.G., Caby, R., Costa, F.G., Cavalcante, J.C., Vasconcelos, A.M., Rodrigues, J.B., 2010. Provenance of the Novo Oriente Group, southwestern Ceará Central Domain, Borborema Province (NE—Brazil): a dismembered segment of a magma-poor passive margin or a restricted rift-related basin? Gondwana Research 18, 497–513.

Araújo, C.E.G., Costa, F.G., Pinéo, T.R.G., Cavalcante, J.C., Moura, C.A.V., 2012. Geochemistry and $^{207}Pb/^{206}Pb$ zircon ages of granitoids from the southern portion of the Tamboril–Santa Quitéria granitic–migmatitic complex, Ceará Central Domain, Borborema Province (NE Brazil). Journal of South American Earth Sciences 33, 21–33.

Araújo, C.E.G., 2014. Evolução tectônica da margem ativa Neoproterozóica do Orógeno Gondwana Oeste na Província Borborema (NE-Brasil) PhD thesis Universidade de São Paulo, 243 p.

Araújo, C.E.G., Cordani, U.G., Weinberg, R.F., Basei, M.A., Armstrong, R., Sato, K., 2014. Tracing Neoproterozoic subduction in the Borborema Province (NE—Brazil): Clues from U–Pb geochronology and Sr–Nd–Hf–O isotopes on granitoids and migmatites. Lithos 202–203, 167–189.

Archanjo, C.J., Viegas, L.G.F., Hollanda, M.H.B.M., Souza, L.C., Liu, D., 2013. Timing of the HT/LP transpression in the Neoproterozoic Seridó Belt (Borborema Province, Brazil): constraints from UPb (SHRIMP) geochronology and implications for the connections between NE Brazil and West Africa. Gondwana Research 23, 701–714.

Arenas, R., Abati, J., Catalán, J.R.M., Garcia, F.D., Pascual, F.J.R., 1997. P–T evolution of eclogites from the Agualada Unit (Ordenes Complex, northwest Iberian Massif, Spain): implications for crustal subduction. Lithos 40, 221–242.

Arthaud, M.H., Caby, R., Fuck, R.A., Dantas, E.L., Parente, C.V., 2008. Geology of the northern Borborema Province, NE Brazil and its correlation with Nigeria, NW Africa. In: Pankhurst, R.J., Trouw, R.A.J., Brito Neves, B.B., de Wit, M.J. (Eds.), West Gondwana: Pre-Cenozoic Correlation Across the South Atlantic Region. Geological Society of London 294, pp. 49–67.

Attoh, K., Morgan, J., 2004. Geochemistry of high-pressure granulites from the Pan-African dahomeyide orogen, West Africa: constraints on the origin and composition of the lower crust. Journal of African Earth Sciences 39, 201–208.

Blichert-Toft, J., Albarède, F., 1997. The Lu-Hf isotope geochemistry of chondrites and the evolution of the mantle-crust system. Earth Planetary Science Letters 148, 243–258. Erratum. Earth Planetary Science Letters 154, 349.

Blichert-Toft, J., Chauvel, C., Albarède, F., 1997. Separation of Hf and Lu for high-precision isotope analysis of rock samples by magnetic sector-multiple collector ICP-MS. Contributions to Mineralogy and Petrology 127, 248–260.

Brito Neves, B.B., Van Schmus, W.R., Fetter, A.H., 2002. Northwestern Africa–Northeastern Brazil: major tectonic links and correlation problems. Journal of African Earth Sciences 34, 275–278.

Bühn, B., Pimentel, M.M., Matteini, M., Dantas, E.L., 2009. High spatial resolution analysis of Pb and U isotopes for geochronology by laser ablation multi-collector inductively coupled plasma mass spectrometry (LA-MC-ICP-MS). Anais da Academia Brasileira de Ciências 81, 99–114.

Caby, R., 1989. Precambrian terranes of Benin Nigéria and Northeast Brazil and the Late Proterozoic South Atlantic. In: Dallmeyer, R.D. (Ed.), Terranes in the Circum-Atlantic Paleozoic Orogens. Geological Society of America Special Papers 230, pp. 145–158.

Caby, R., 2003. Terrane assembly and geodynamic evolution of central–western Hoggar: a synthesis. Journal of African Earth Sciences 37, 133–159.

Caby, R., Buscail, F., Dembele, D., Diakite, S., Sacko, S., Bal, M., 2008. Neoproterozoic garnet-glaucophanites and eclogites: new insights for subduction metamorphism of the Gourma fold and thrust belt (eastern Mali). In: Ennih, N., Liégeois, J.-P. (Eds.), The Boundaries of the West African Craton. Geological Society of London, Special Publications 297, pp. 203–216.

Carswell, D.A., Zhang, R.Y., 1999. Petrographic characteristics and metamorphic evolution of ultrahigh-pressure eclogites in plate-collision belts. International Geology Review 41, 781–798.

Castaing, C., Feybesse, J.L., Thié Blemont, C., Triboulet, C., Chevremont, P., 1994. Paleogeographical reconstructions of the Pan-Africano/Brasiliano Orogen: closure of an oceanic domain or intracontinental convergence between major blocks? Precambrian Research 69, 327–344.

Castro, N.A., 2004. Evolução geológica proterozóica da região entre Madalena e Taperuaba, Domínio Tectônico Ceará central — Província Borborema(PhD thesis) Institute of Geoscience, São Paulo University, (220 pp.).

Cavalcante, J.C., Vasconcelos, A.M., Medeiros, M.F., Paiva, I.P., Gomes, F.E.M., Cavalcante, S.N., Cavalcante, J.E., Melo, A.C.R., Duarte Neto, V.C. & Benevides, H.C. 2003. Mapa Geológico do Estado do Ceará – Escala 1:500.000. Fortaleza, Ministério das Minas e Energia, CPRM.

Chauvel, C., Blichert-Toft, J.E., 2001. A hafnium isotope and trace element perspective on melting of the depleted mantle. Earth and Planetary Science Letters 190, 137–151.

Cheng, H., Nakamura, E., Kobayashi, K., Zhou, Z., 2007. Origin of atoll garnets in eclogites and implications for the redistribution of trace elements during slab exhumation in a continental subduction zone. American Mineralogist 92, 1119–1129.

Chopin, C., 2003. Ultrahigh-pressure metamorphism: tracing continental crust into the mantle. Earth and Planetary Science Letters 212, 1–14.

Cordani, U.G., Teixeira, W., D'Agrella-Filho, M.S., Trindade, R.I., 2009. The position of the Amazonian Craton in supercontinents. Gondwana Research 15, 396–407.

Cordani, U.G., Pimentel, M.M., Araújo, C.E.G., Basei, M.A.S., Fuck, R.A., Girardi, V.A.V., 2013a. Was there an Ediacaran Clymene ocean in central South America? American Journal of Sciences 313, 517–539.

Cordani, U.G., Pimentel, M.M., Araújo, C.E.G., Fuck, R.A., 2013b. The significance of the Transbrasiliano-Kandi tectonic corridor for the amalgamation of West Gondwana. Brazilian Journal of Geology 43, 583–597.

Corfu, F., Hanchar, J.M., Hoskin, P.W.O., Kinny, P.D., 2003. An atlas of zircon textures. In: Hanchar, J.M., Hoskin, P.W.O. (Eds.), ZirconReviews of Mineralogy and Geochemistry 53. Mineralogical Society of America, Washington, D.C., pp. 469–500.

da Silva, L.C., Armstrong, R., Pimentel, M.M., Scandolara, J., Ramgrab, G., Wildner, W., Angelim, L.A.A., Vasconcelos, A.M., Rizzoto, G., Quadros, M.L.E.S., Sander, A., Rosa, A.L.Z., 2002. Reavaliação da evolução geológica em terrenos pré-cambrianos brasileiros com base em novos dados U–Pb SHRIMP, Parte III: Províncias Borborema, Mantiqueira Meridional e Rio Negro-Juruena. Revista Brasileira de Geociencias 32, 529–544.

Duclaux, G., Ménot, R.P., Guillot, S., Agbossoumondé, Y., Hilairet, N., 2006. The mafic layered complex of the Kabyé massif (north Togo and north Benin): evidence of a Pan-African granulitic continental arc root. Precambrian Research 151, 101–118.

El-Hadj Tidjani, M., Affaton, P., Louis, P., Socohou, A., 1997. Gravity characteristics of the Pan-African Orogen in Ghana, Togo and Benin (West Africa). Journal of African Earth Sciences 24, 241–258.

Ernst, W.G., 2001. Subduction, ultrahigh-pressure metamorphism, and regurgitation of buoyant crustal slices — implications for arcs and continental growth. Physics of the Earth and Planetary Interiors 127, 253–275.

Fetter, A.H., 1999. U–Pb and Sm–Nd Geochronological Constraints on the Crustal Framework and Geologic History of Ceará State, NW Borborema Province, NE Brazil: Implications for the Assembly of Gondwana(PhD thesis) Department of Geology, University of Kansas, (164 pp.).

Fetter, A.H., Van Schmus, W.R., Santos, T.J.S., Nogueira Neto, J.A., Arthaud, M.H., 2000. U–Pb and Sm–Nd geochronological constraints on the crustal evolution and basement architecture of Ceará State, NW Borborema Province, NE Brazil: implications for the existence of the Paleoproterozoic Supercontinent "Atlantica". Revista Brasileira de Geociencias 30, 102–106.

Fetter, A.H., Santos, T.J.S., Van Schmus, W.R., Hackspacher, P.C., Brito Neves, B.B., Arthaud, M.H., Nogueira Neto, J.A., Wernick, E., 2003. Evidence for Neoproterozoic continental arc magmatism in the Santa Quitéria Batholith of Ceará State, NW Borborema Province, NE Brazil: implications for the assembly of West Gondwana. Gondwana Research 6, 265–273.

Garcia, M.G.M., Santos, T.J.S., Amaral, W.S., 2014. Provenance and tectonic setting of neoproterozoic supracrustal rocks from the Ceará Central Domain, Borborema Province (NE Brazil): constraints from geochemistry and detrital zircon ages. International Geology Review 56 (4), 481–500. http://dx.doi.org/10.1080/00206814.2013.875489.

Ghiribelli, B., Frezzotti, M.-L., Palmeri, R., 2002. Coesite in eclogites of the Lanterman Range (Antarctica): evidence from textural and Raman studies. European Journal of Mineralogy 14, 355–360.

Griffin, W.L., Wang, X., Jackson, S.E., Pearson, N.J., O'Reilly, S.Y., Xu, X., Zhou, X., 2002. Zircon chemistry and magma mixing, SE China: in-situ analysis of Hf isotopes, Tonglu and Pingtan igneous complexes. Lithos 61, 237–269.

Harley, S.L., Kelly, N.M., Möller, A., 2007. Zircon behaviour and the thermal histories of mountain chains. Elements 3, 25–30.

Jackson, S.E., Pearson, N.J., Griffin, W.L., Belousova, E.A., 2004. The application of laser ablation inductively coupled plasma-mass spectrometry to in situ U–Pb zircon geochronology. Chemical Geology 211, 47–69.

Jahn, B.-M., Caby, R., Monié, P., 2001. The oldest UHP eclogites of the world: age of UHP metamorphism, nature of protoliths and tectonic implications. Chemical Geology 178, 143–158.

Kalsbeek, F., Affaton, P., Ekwueme, B., Frei, R., Thrane, K., 2012. Geochronology of granitoid and metasedimentary rocks from Togo and Benin, West Africa: comparisons with NE Brazil. Precambrian Research 196–197, 218–233.

Lesquer, A., Beltrão, J.F., Abreu, F.A.M., 1984. Proterozoic links between Northeastern Brazil and West Africa: a plate tectonic model based on gravity data. Tectonophysics 110, 9–26.

Liu, J., Ye, K., Sun, M., 2006. Exhumation P – T path of UHP eclogites in the Hongan area, western Dabie Mountains, China. Lithos 89, 154–173.

Lu, Z., Zhang, L., Du, J., Bucher, K., 2008. Coesite inclusions in garnet from eclogitic rocks in western Tianshan, northwest China: convincing proof of UHP metamorphism. American Mineralogist 93, 1845–1850.

Ludwig, K.R., 2003. Isoplot 3.0 — a geochronological toolkit for Microsoft Excel. Berkeley Geochronology Center Special Publication 4, 1–70.

Martins, G., Oliveira, E.P., Lafon, J.-M., 2009. The Algodões amphibolite–tonalite gneiss sequence, Borborema Province, NE Brazil: geochemical and geochronological evidence for Palaeoproterozoic accretion of oceanic plateau/back-arc basalts and adakitic plutons. Gondwana Research 15, 71–85.

Maruyama, S., Liou, J.G., Terabayashi, M., 1996. Blueschists and eclogites of the world and their exhumation. International Geology Review 38, 485–594.

Matteini, M., Dantas, E.L., Pimentel, M.M., Bühn, B., 2010. Combined U – Pb and Lu – Hf isotope analyses by laser ablation MC-ICP-MS: methodology and applications. Anais da Academia Brasileira de Ciências 82, 479–491.
Monié, P., Caby, R., Arthaud, M.H., 1997. The Neoproterozoic Brasiliano Orogeny in Northeast Brazil: 40Ar/39Ar and petrostructural data from Ceará. Precambrian Research 81, 241–264.
Morel, M.L.A., Nebel, O., Nebel-Jacobsen, Y.L., Miller, J.S., Vroon, P.Z., 2008. Hafnium isotope characterization of the GJ-1 zircon reference material by solution and laser-ablation MC-ICPMS. Chemical Geology 255, 231–235.
Morishita, T., Arai, S., Gervilla, F., 2001. High-pressure aluminous mafic rocks from the Ronda peridotite massif, southern Spain: significance of sapphirine- and corundum-bearing mineral assemblages. Lithos 57, 143–161.
Nogueira Neto, J.A., Fetter, A.H., Legrand, J.M., Santos, T.J.S., Hackspacher, P.C., 1997. Idade Neoproterozóica em Granulitos de Cariré (NW do Ceará): U/Pb em Titanita e Idade Modelo (TDM) — Resultados Iniciais. SBG, Simpósio Nacional de Estudos Tectônicos 6, pp. 101–103 (Pirenópoles).
O'Brien, P.J., Ziemann, M.A., 2008. Preservation of coesite in exhumed eclogite: insights from Raman mapping. European Journal of Mineralogy 20, 827–834.
Pimentel, M.M., Fuck, R.A., 1992. Neoproterozoic crustal accretion in central Brazil. Geology 20, 375–379.
Pimentel, M.M., Heaman, L.M., Fuck, R.A., 1991. Zircon and sphene U–Pb geochronology of Upper Proterozoic volcanic-arc rock units from southwestern Goiás, central Brazil. Journal of South American Earth Sciences 4, 295–305.
Pimentel, M.M., Fuck, R.A., Jost, H., Filho, C.F.F., 2000. The basement of the Brasilia Fold Belt and the Goiás Magmatic Arc. In: Cordani, U.G., Milani, E.J., Thomaz-Filho, A., Campos, D.A. (Eds.), Tectonic Evolution of South America. Brazil, Rio de Janeiro, pp. 195–229.
Pimentel, M.M., Rodrigues, J., DellaGiustina, M.E., Junges, S., Matteini, M., Armstrong, R., 2011. The tectonic evolution of the Neoproterozoic Brasilia Belt, central Brazil, based on SHRIMP and LA-ICPMS U-Pb sedimentary provenance data: a review. Journal of South American Earth Sciences 31, 345–357.
Rubatto, D., 2002. Zircon trace element geochemistry: partitioning with garnet and the link between U–Pb ages and metamorphism. Chemical Geology 184, 123–138.
Rubatto, D., Gebauer, D., 2000. Use of cathodoluminescence for U–Pb zircon dating by ion microprobe: some examples from the Western Alps. In: Pagel, M., Barbin, V., Blanc, P., Ohnenstetter, D. (Eds.), Cathodoluminescence in Geosciences. Springer, Berlin, pp. 373–400.
Santos, T.J.S., Fetter, A.H., Hackspacher, P.C., Van Schmus, W.R., Nogueira Neto, J.A., 2008a. Neoproterozoic tectonic and magmatic episodes in the NW sector of Borborema Province, NE Brazil, during assembly of Western Gondwana. Journal of South American Earth Sciences 25, 271–284.
Santos, T.J.S., Fetter, A.H., Nogueira Neto, J.A., 2008b. Comparisons between the northwestern Borborema Province, NE Brazil, and the southwestern Pharusian Dahomey Belt, SW Central Africa. In: Pankhurst, R.J., Trouw, R.A.J., Brito Neves, B.B., de Wit, M.J. (Eds.), West Gondwana: Pre-Cenozoic Correlation Across the South Atlantic Region. Geological Society, London, Special Publications 294, pp. 101–120.
Santos, T.J.S., Fetter, A.H., Van Schmus, W.R., Hackspacher, P.C., 2009a. Evidence for 2.35 to 2.30 Ga juvenile crustal growth in the northwest Borborema Province, NE Brazil. In: Reddy, S.M., Mazunder, R., Evans, D.A.D., Collins, A.S. (Eds.), Palaeoproterozoic Supercontinents and Global Evolution. Geological Society, London, Special Publications 323, pp. 271–281.
Santos, T.J.S., Garcia, M.G.M., Amaral, W.S., Caby, R., Wernick, E., Arthaud, M.H., Dantas, E.L., Santosh, M., 2009b. Relics of eclogite facies assemblages in the Ceará Central Domain, NW Borborema Province, NE Brazil: implications for the assembly of West Gondwana. Gondwana Research 15, 454–470.
Scherer, E., Münker, C., Mezger, K., 2006. Calibration of the lutetium–hafnium clock. Science 293, 683–687.
Schreyer, W., 1995. Ultrahigh metamorphic rocks: the retrospective viewpoint. Journal of Geophysical Research 100, 8353–8366.
Shimpo, M., Tsunogae, T., Santosh, M., 2006. First report of garnet–corundum rocks from southern India: implications for prograde high-pressure (eclogite-facies?) metamorphism. Earth and Planetary Science Letters 242, 111–129.
Stacey, S., Kramers, J.D., 1975. Approximation of terrestrial lead isotope evolution by a two stage model. Earth and Planetary Science Letters 26, 2027–2221.
Tohver, E., D'Agrella-Filho, M.S., Trindade, R.I.F., 2006. Paleomagnetic record of Africa and South America for the 1200–500 Ma interval, and evaluation of Rodinia and Gondwana assemblies. Precambrian Research 147, 193–222.
Trompette, R., 1994. Geology of Western Gondwana, Pan-African - Brasiliano aggregation of South America and Africa. Brookfield, A. A. Balkema, Rotterdam, 350 pp.
Trompette, R., 2000. Gondwana evolution; its assembly at around 600 Ma. Earth and Planetary Sciences 330, 305–315.
Valeriano, C.M., Pimentel, M.M., Heilbron, M., Almeida, J.C.H., Trouw, R.A.J., 2008. Tectonic evolution of the Brasília Belt, Central Brazil, and early assembly of Gondwana. In: Pankhurst, R.J., Trouw, R.A.J., Brito Neves, B.B., de Wit, M.J. (Eds.), West Gondwana: Pre-Cenozoic Correlation Across the South Atlantic Region. Geological Society, London, Special Publications 294, pp. 197–210.
Van der Pluijm, B.A., Marshak, S., 1997. Earth Structure: An Introduction to Structural Geology and Tectonics. McGraw-Hill.
Viegas, L.G.F., Archanjo, C.J., Vauchez, A., 2014. Microfabrics and zircon U–Pb (SHRIMP) chronology of mylonites from the Patos shear zone (Borborema Province, NE Brazil). Precambrian Research 243, 1–17.
Zhang, L.F., Song, S., Liou, J.G., Ai, Y., Li, X., 2005. Relict coesite exsolution in omphacite from Western Tianshan eclogites, China. American Mineralogist 90, 181–186.